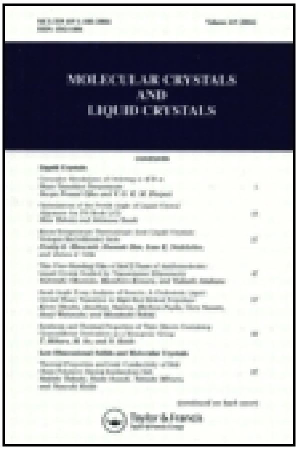

Molecular Crystals and Liquid Crystals
Publication details, including instructions for authors and subscription information:
http://www.tandfonline.com/loi/gmcl16

Application of the Particle in the Box Model for Resonance Raman Scattering to Recent Experimental Results of Poly-Acetylene

H. Kuzmany [a] & P. Knoll [a]
[a] Institut für Festkörperphysik der Universität Wien and Ludwig Boltzraann Institut für Festkörperphysik, A-1090, Vienna, Austria

To cite this article: H. Kuzmany & P. Knoll (1985): Application of the Particle in the Box Model for Resonance Raman Scattering to Recent Experimental Results of Poly-Acetylene, Molecular Crystals and Liquid Crystals, 117:1, 385-392

To link to this article: http://dx.doi.org/10.1080/00268948508074656

Mol. Cryst. Liq. Cryst. 1985, Vol. 117, pp. 385-392
0026-8941/85/1174-0385/$15.00/0

Printed in the United States of America

APPLICATION OF THE PARTICLE IN THE BOX MODEL FOR RESONANCE RAMAN SCATTERING TO RECENT EXPERIMENTAL RESULTS OF POLYACETYLENE

H. KUZMANY AND P. KNOLL
Institut für Festkörperphysik der Universität Wien and
Ludwig Boltzmann Institut für Festkörperphysik,
A-1090 Vienna/ Austria

Abstract The resonance Raman effect of trans polyacetylene is described in terms of a photoselective resonance scattering from a distribution of conjugation lengths. Higher excited states of the π-π^*-transition are included and very good agreement with experimental results is obtained with respect to scattering intensity and line width if a strong inhomogenious broadening of the vibronic oscillator is assumed. For a high quality sample 85 % of the polymer is in segments longer than 20 double bonds. Application of the model to isomerization and electrochemical doping shows that both processes start in the highly disordered areas.

1. INTRODUCTION

Polyacetylene has been treated so far as a quasi one-dimensional Peierls insulator with extended electronic states. Recently several experiments showed that the π-electron system is frequently disturbed by defects on the conjugations.[1,2] Thus, the electrons are confined to certain regions on the chain and the polymer should be regarded as a particle in the box system with a statistical distribution of boxlengths corresponding to the regions of undisturbed conjugations. This picture had been suggested previously from an analysis of the resonance Raman effect in trans - polyacetylene[3,4]. In this case the electronic properties of the individual segments are similar to those of oligoenes and the observed experimental result is a consequence of a photoselective resonance process. Thus, a careful analysis of Raman data provides a useful tool to study the micromorphology of the chains. One disadvantage of the methode originats from several crude assumptions used so far for the evaluation of the resonance Raman effect. Thus, the originally evaluated mean conjugation length of 30 double bonds[3] had been questioned by results ranging from very short conjugations[4] to quasi infinite chains.[5] Very recently strong progress was obtained in the theoretical treatment of the problem[6-8] and a satisfactory description of the problem is now available. Very good agreement between calculated and observed line shapes is obtained. Thus, the methode of analysis is ready for applications to specific problems like cis-trans isomerization, degradation, electrochemical cycling ect. Details of the model calculations have been summarized recently in a review article by one of the authors.[9]

2. THE PARTICLE IN THE BOX MODEL

To evaluate the Raman line shapes and Raman intensities for trans-polyacetylene an individual undisturbed segment of the chain has to be studied first. The result must be weight averaged by the distribution of conjugation lengths P(N). The resonance Raman effect of the individual segments can be described by the Albrecht theory using the Franck - Condon approach for the evaluation of the excited state wave functions.

The Raman cross section is given as

$$\left(\frac{d^2\sigma}{d\Omega d\omega}\right)_{m,n} = \frac{2\ \omega_s^3}{3^2 c^4 \hbar} \sum_{\rho,\sigma} |\alpha_{\rho\pi}|^2 \tag{1}$$

where $\alpha_{\rho\sigma}$ is the ρ,σ component of the transition polarizability and the intensity of the scattered light is given in counts per second. Within the above described approach $\alpha_{\rho\sigma}$ yields for the first order Raman process of vibronic state s and an electronic transition along the chain axis (z-axis)

$$\alpha_{zz} = \sum_I \rho_{ge}^2 \sum_v \frac{\langle 0|v\rangle\langle v|1_s\rangle}{\varepsilon_{Iv} - \varepsilon_o + i\Gamma_e/2} \tag{2}$$

where ρ_{ge}, ε_o and Γ_e are the pure electronic transition matrix element between the electronic ground and excited state, the energy of the exciting light and the damping constant for the electronic oscillator, respectively. ε_{Iv} is the electronic transition energie between ground state and excited state including contributions from the vibrations. The Franck - Condon integrals $\langle 0|v\rangle\langle v|1_s\rangle$ can be evaluated analytically in terms of coupling constants a_i. Thus, using a Lorentzian or Gaussian line shape $L(\nu,\Gamma_p)$ with a vibronic damping constant Γ_p allows to evaluate the experimentally observed Raman intensity after weight averaging. Since the spatial extension of the laserfocus is definitely larger than most of the segments the latter may be considered as individual scatterers and no normalization to scattering volume is necessairy.

The electronic properties of the segments like ε_{Iv} or $\rho_{ge} = \rho_I$ can be evaluated within the Hückel theory.[8] The calculation showed that in the case of resonance the lowest π-π^* transition gives the strongest contribution to the scattering process but transitions with higher energies are not negligible. They may even

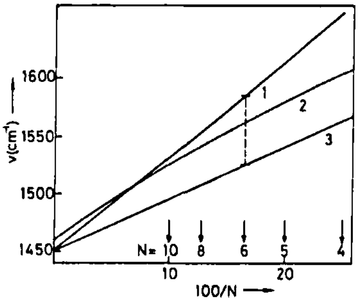

FIGURE 1 Vibrational frequencies **versus inverse** segment length; 1 carotenoides[10], 2 (Ref.3) 3 average of various oligoenes.[4]

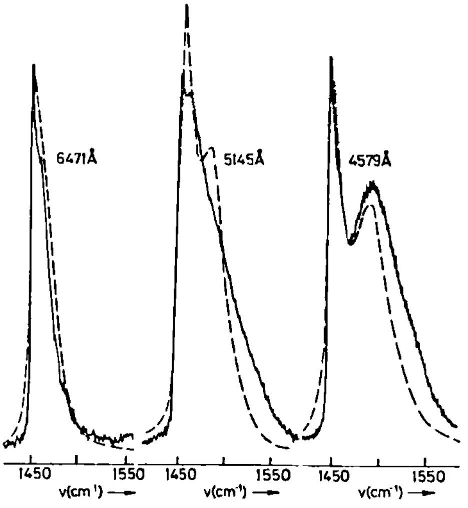

FIGURE 2 Calculated (---) and experimental (——) Raman line shaped for $\nu_{C=C}$

contribute in resonance for an exciting laser energy larger than the lowest π-π^* transition. The matrix element ρ_I exhibites a strong dependence on the transition energy which for long segments approaches $\rho_I \propto 1/\varepsilon_I^2$. As a consequence it also depends strongly on the lengths of the segments. Since it **enters** as ρ_I^4 into the scattering intensity it plays a dominating role for the evaluation of the distribution.

With respect to the vibrations only the C=C stretch mode around 1500 cm^{-1} (1) and the mode around 1100 cm^{-2} (2) have to be considered for the evaluation of the Frank - Condon integrals. Their dependence on N may be obtained from empirical relations observed for several oligoenes like carotenoides, diphenylpolyenes or dicarboxylic ester polyenes. These relations have the general form

$$\nu_i = A_i + B_i/N \quad \text{or} \quad \nu_i = A_i + B_i/(N + 1) \qquad (3)$$

Fig.1 shows some of these relations for the C=C stretch mode as used by various authors.[3,4,10] The discrepancy is a consequence of the various oligoenes. The difference in observed frequencies increases with decreasing length of the segment. For N=6 it has e.g. an approximate value of 60 cm^{-1}.

Fig.2 shows a best fit calculation of Raman lines for the C=C stretch mode $\nu_{C=C}$ in high quality trans-polyacetylene in comparison to experimental results for three laser lines. Calculated and experimentally observed intensities have only been matched for the peak of the line excited with the red laser. Very good agreement is observed for the selected laser lines which implies that also the excitation profile over the whole visible spectral range will be reproduced satisfactoringly. The discrepancy between calculated and observed intensities is likely to be due to uncertainties in the calibration of the spectrometer. For the calculation the dependence of the electronic and vibrational damping constant on N was considered phenomenologically by a relation similar to Eq.3 and the Frank - Condon coupling constants were evaluated from $a(N) = C(1 + 9.5/N)$ (Ref.9). For the distribution function a bimodal log normal distribution with the parameters N_i, Δ_i and F_i for the peak, width and relative weight, respectively was used. Tab.1 summarizes the parameters for the evaluation of the dashed lines in Fig.2.

TABLE 1 Parameters values for high quality trans-polyacetylene

P(N)			$\nu_1(N)$	$\nu_2(N)$	$\Gamma_p(N)$	$\Gamma_e(N)$	a(N)
$F_1=0.6$	$N_1=10$	$\Delta_1=0.8$	$A_1=1050$	$A_2=1450$	$A_p=6$	$A_e=1200$	$C=0.2$
$F_2=0.4$	$N_2=50$	$\Delta_2=0.4$	$B_1=350$	$B_2=460$	$B_p=360$	$B_e=-1800$	

3. DISCUSSION OF THE PARAMETERS

The vibrational damping Γ_p is determined by the two constants A_p and B_p. From the very steep edge on the low frequency side of the Raman lines A_p can definitely not be larger than 6 cm^{-1}. On the other hand in order to describe properly the broad wing of the lines B_p must be as large as 360 which yields a damping constant of e.g. 60 cm^{-1} for N=6. A comparison with Fig.1 shows, that this is obviously an inhomogeneuous broadening rather than a life time broadening. One can show explicitely, that instead of using the large value for B_p a corresponding large range of B may be used.

An additional mechanism for the broadening of the Raman lines comes from the violation of momentum selection rules for the Raman process in very short segments. For such segments the q-vectors of the modes are not good quantum numbers any more and modes with $q \neq 0$ may contribute to the scattering process. A classical treatment of the problem on the basis of interference yields a correction factor for the scattering intensities for $q \neq 0$ modes of the form

$$f = \frac{1 - \cos(N.a(k_s - k_i + q))}{1 - \cos((k_s - k_i + q)a)} \approx \frac{1 - \cos(\pi n)}{1 - \cos(\pi n/N)} \qquad (4)$$

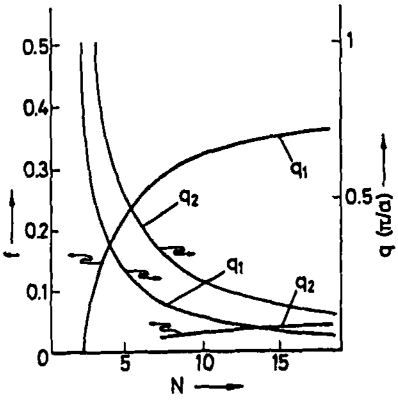

FIGURE 3 Wave vectors q and correction factor f for scattering from q≠0 vibrational modes.

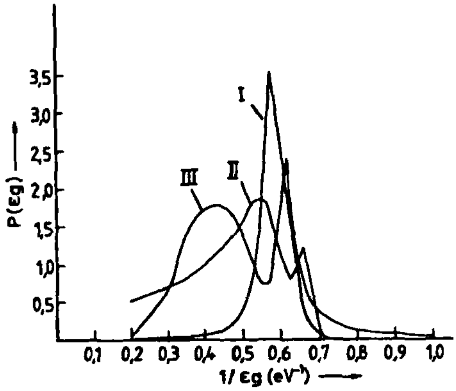

FIGURE 4 Distribution of gap energies calculated from P(λ) and P(N).

where k_s and k_i are the incident and scattered light wave vectors, respectively. As compared to f=1 for q=0 Fig.3 shows f for the first two q-vectors q_1 and q_2 not equal zero, together with the magnitude of these vectors as a function of segment length N. For large values of N f can be substantially different from zero at least for q_1. However, in this case q is very small and the corresponding vibrational frequency will be identical to the one for q=0. For large values of q (small values of N) f decreases rapidly to zero. Thus only in the limited range from $4 \leq N \leq 15$ a contribution of q≠0 modes can be expected.

The distribution function has a large and broad peak around N=50 and a smaller and narrower peak around N=10. The total amount of material in segments longer than e.g. 20 double bonds is larger than 80 %. These values are in good agreement with x-ray results concerning coherence lengths and crystallinity.[11] In order to compare the result with other experiments it must be kept in mind that P(N) is a distribution of segments rather than a distribution of material in the segments. The latter distribution is obtained by multiplying P(N) with N. Vardeny et al.[5] recently described the resonance Raman lines in trans-polyacetylene by a distribution of electron-phonon coupling constant λ rather than by a distribution of segment lengths. Since in the particle in the box model any distribution of segment lengths immediately leads to a distribution in coupling constants a(N) there are definitely close relations between the two models. Using e.g. in case of Ref.5 the gap equation

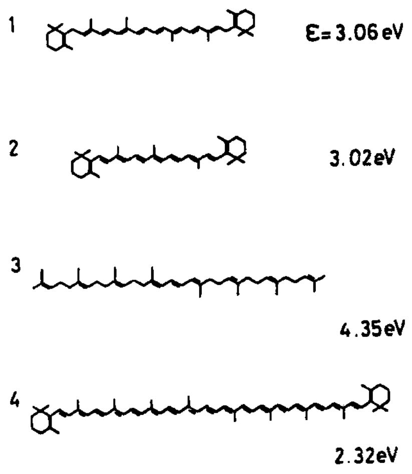

FIGURE 5 Interruption of conjugations in oligoemes.

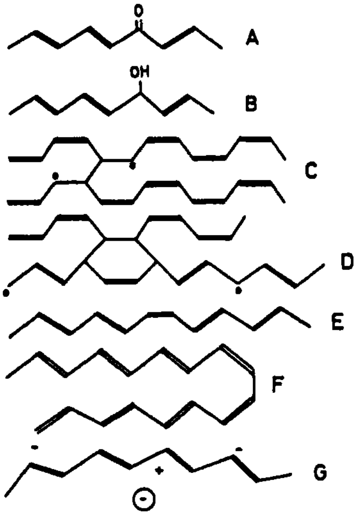

FIGURE 6 Possible type of defects with strong and weak interruptions of conjugations.

$$\varepsilon_g = 4\, E_c \exp(\, - 1/2\lambda), \quad E_c = 6.3 \text{ eV} \qquad (5)$$

and in our case the particle in the box equation

$$\varepsilon_g = V_o + h^2/16\, m_o a^2 N \qquad (5a)$$

to evaluate the optical transition energies, both cases yield a distribution in optical transition energies ε . Fig.4 shows results for the distributions reported in Ref.5 (curve I) and in Ref.7 (curve II) in comparison to the distribution reported in this work (curve III). Keeping in mind the weak significance for the exact position of the long segment peak because of the solid state limit the agreement between results of Ref.7 and our results is satisfactoring. The results of Ref.5 also agree roughly with the long segment peak but the distribution from the short segments is missing. As a tentative explanation for the discrepancy ρ_I used in the two models may have a different energy dependence. As a matter of fact performing a fit similar to the one shown in Fig.2 with ρ_I independent of ε_I yields distribution in gap energies similar to the results of Ref.5.

The question refering to the nature of an interruption of the conjugations may be discussed considering finite polyenes as demonstrated in Fig.5. Compound 1 (dihydro β-carotene) has 10 double bonds and an optical transition ε = 3.06 eV. Compound 2 (septareno β-carotene) has 9 double bonds but ε is only 3.02 eV. The discrepancy arrises from the interruption of the last conjugations at the end by two single bonds. The length of the undisturbed segment is only 8 double bonds. This effect is even more dramatically demonstrated for trans-phytoene (3). This compound has 9 double bonds but only 3 are uninterrupted. Thus ε becomes as large as 4.35 eV. Finally compound 4 (dodecapreno β-carotene) has 19 uninterrupted double bonds and consequently ε is only 2.32 eV. Fig.6 shows examples for possible interruptions of conjugations in polyacetylene. The defects A to D (carbonyl group, hydroxyl group, simple cross link, Diels Alder cross link after partial isomerization, respectively) refer to a complete interruption of conjugations in the sense of Fig.5 whereas defects E to G (quenched cis-segment, chain fold, chain bending or twisting and polarization defects, respectively) will only provide a weak disturbance of the π-electron system. Weak disturbances of the conjugations have recently been observed to cause a similar but less effective change of electronic transition energies and transition matrix elements as compared to complete interruptions[12].

4. APPLICATIONS

Though the resonance Raman effect and the shape of the Raman lines are now well understood. Details of the nature of most of the defects are completely unknown. Artificial degradation of the samples is one way to learn about it. It was e.g. shown, that exposure of polyacetylene to air changes the relative hight of the low frequency and the high frequency part of the C=C stretch mode line if excited with blue laser light. However the effect is surprisingly weak and has a time constant of several days[13]. Compactation[13] or irradiation with laser light[14] are other possibilities for an artificial sample degradation. The most homogeneous and, therefore, the best way to obtain a well defined lineshape appears to be over isomerization. However, because of the lack of a satisfactoring theory so far most of these experiments have been analysed only qualitatively.

Cis-trans isomerization studies are an other type of experiments, where the analysis of the Raman lines yields information about the material. During thermal isomerization short segments were observed to isomerize first with a lower activation energy. Thus the trans-fraction in a nominally cis-polymer always consists of predominantly short segments. Electrochemical doping experiments showed that this part of the samples dopes first. Furthermore, doping a cis-polymer leads to a complete cis-trans isomerization and the obtained trans-polymer shows a very low concentration of short segments. However, as a consequence of subsequent doping - undoping cycles this concentration increases continously. Doping trans-polyacetylene electrochemically it was observed that the peak for the short segments decreases first. Thus, doping starts in the highly disordered areas. Details of the electrochemical doping experiments are reported in the paper of Müller et al.[15] in these proceedings.

5. CONCLUSION

In conclusion the particle in the box model represents a satisfactoring model to describe the resonance Raman effect in trans-polyacetylene. The analysis of the line shapes of the Raman lines allows to determine the distribution function for the segments with undisturbed conjugations. This possibility turns out to be of increasing importance for the analysis of solid state reactions in the polymer like e.g. isomerization and electrochemical doping.

Acknowledgement This work was supported by the "Stiftung Volkswagenwerk".

REFERENCES

1. T.C. Clarke, R.D. Kendrick and C.S. Yanoni, J. de Physique 44-C3, 369 (1983).
2. M. Mehring, H. Seidl, W. Müller and G. Wegner, Solid State Communic. 45, 1075 (1983).
3. H. Kuzmany, phys. stat. sol. (b) 97, 521 (1980).
4. L.S. Lichtmann, Ph. D. Thesis, Cornell University 1981.
5. Z. Vardeny, E. Ehrenfreund, O. Brafman and B. Horovitz, Phys. Rev. Lett. 51, 2326 (1983).
6. H. Kuzmany, E.A. Imhoff, D.B. Fitchen and A. Sarhangi, Phys. Rev. B, 26, 7109 (1982).
7. G.P. Brivio and E. Mulazzi, Chem. Phys. Lett. 95, 555 (1983).
8. H. Kuzmany, P.R. Surjan and M. Kertêsz, Solid State Communic. 48, 243 (1983).
9. H. Kuzmany, J. of Pure and Applied Chemistry (to be published).
10. L. Rimai, M.E. Heyde and D. Gill, J. Am. Chem. Soc. 93, 4493 (1973).
11. J.P. Pouget, R. Robin, R. Comes, H.W. Gibson, A.J. Epstein and D. Billand, Physica, (to be published).
12. P. Surjan, K. Iwahana and H. Kuzmany (unpublished).
13. P. Knoll and H. Kuzmany, Mol. Cryst. Liq. Cryst. 106, 317 (1984).
14. P. Knoll, K. Iwahana and H. Kuzmany, Mol. Cryst. Liq. Cryst. (this volume).
15. F. Müller, P. Meisterle and H. Kuzmany, Mol. Cryst Liq. Cryst. (this volume).